# Radiative lifetime of metastable $2^3S_1$ $Li^+$

R. D. Knight* and M. H. Prior
*Department of Physics, University of California, and Lawrence Berkeley Laboratory, Berkeley, California 94720*
(Received 17 September 1979)

The radiative lifetime of $1s2s\,^3S_1$ $Li^+$ ions has been measured by a comparison of the count rate of spontaneous decay photons (210 Å) to a laser-induced fluorescence signal proportional to the total number of metastable ions. The ions were confined in a rf-quadrupole trap, and the fluorescence signal used was the intercombination transition $1s2p\,^3P_1$ to $1s^2\,^1S_0$ at 202 Å. The $^3P_1$ state was populated from $^3S_1$ by absorption of laser photons at 5485 Å. The result is $\tau_r = 58.6 \pm 12.9$ sec (95% confidence level); theory predicts $\tau_r = 49.1$ sec.

## I. INTRODUCTION

The two-electron atom is one of the simplest systems in atomic physics. Understanding of such systems can be gauged by the remarkable precision with which the energy levels and other properties can be calculated. It is quite surprising, then, that the dominant decay mode of the lowest excited state ($1s2s\,^3S_1$) was not discovered until 1969. In that year, Gabriel and Jordan[1] reported the observation of emission lines in the solar x-ray spectrum which they attributed to single-photon decay of this state in various heliumlike ions. For nearly 30 years prior to this, the $2\,^3S_1$ decay mode had been considered, based on work by Breit and Teller,[2] to be two-photon emission.

Numerous studies of the $2\,^3S_1$ state have occurred since the discovery of single-photon decay. Theoretical work by Griem,[3] followed by the more detailed calculations of Drake[4] and Johnson and Lin,[5] verified that single-photon relativistic magnetic dipole ($M1$) decay is the dominant mechanism. A nonzero transition rate arises from the "finite-wavelength" corrections to the $M1$ operator and can be calculated in the second Pauli approximation. A measurement of the $M1$ decay rate has been reported for He by Woodworth and Moos,[6] and several investigators[7] have made lifetime measurements using the beam-foil time-of-flight technique on two-electron ions with $Z$ in the range $16 \leq Z \leq 36$.

Since the transition rate scales as $Z^{10}$, the lifetimes measured span nearly 14 orders of magnitude (8000 sec at $Z=2$ down to 0.2 nsec at $Z=36$). The agreement of theory and experiment over this exceptionally large range is generally satisfactory. However, the beam-foil experiments[7] observe an apparent nonexponential decay of $2\,^3S_1$ for times less than $\simeq 1$ theoretical lifetime; only when the detector is more than one mean decay length downstream from the foil do the measured decay curves approach single-exponential character with lifetimes in agreement with theoretical values. For shorter foil-detector separations the apparent decay rate is anomalously fast. This behavior is not yet understood, although Lin and Armstrong[8] have suggested an explanation based on the assumed presence of a three-electron-ion component in the beam. The possibility of additional processes affecting the decay of the $2\,^3S_1$ state has not been ruled out. Because of the importance of this transition in astrophysics,[9] possibly as a diagnostic for laboratory plasmas, and as a general test of our understanding of two-electron atoms, a lifetime measurement at $Z=3$ by a completely different technique was judged to be useful.

In this paper we report a measurement of the radiative lifetime of $2\,^3S_1$ in $Li^+$ ions which are stored for many seconds in an ion trap. The theoretical value[4] for the lifetime is 49.0 sec. We determine the lifetime by a comparison of spontaneous $M1$ decay at 210 Å to the intercombination $2\,^3P_1$-$1\,^1S_0$ decay (202 Å) following $2\,^3S_1$-$2\,^3P_1$ excitation at 5485 Å with a dye laser. After discussing the methods and results of our experiment, our measured value is compared with theory and previous measurements.

## II. LIFETIME MEASUREMENT PROCEDURES

In principle, measurement of the metastable lifetime is very straightforward; simply create $Li^+$ ions, some of which are in the $2\,^3S_1$ state, in the ion trap and monitor the metastable population as a function of time. Many difficulties conspire to destroy this simplicity, including imperfect ion storage, poor signal-to-noise for detecting spontaneous emission, and, most important, nonradiative quenching of the metastables. These problems prevented us from determining the radiative lifetime by measuring spontaneous decay curves and led to the adoption of the spontaneous emission-intercombination line comparison de-

 

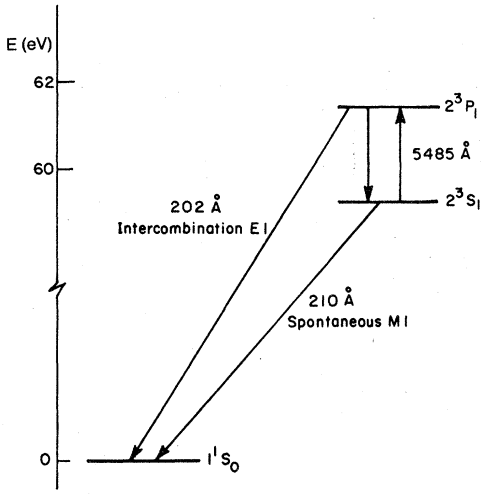


FIG. 1. Relevant low-lying energy levels of $Li^+$. Laser light at 5485 Å excites ions in the $2\,^3S_1$ state to $2\,^3P_1$, from which intercombination radiation at 202 Å is emitted in about 0.1% of the subsequent decays.

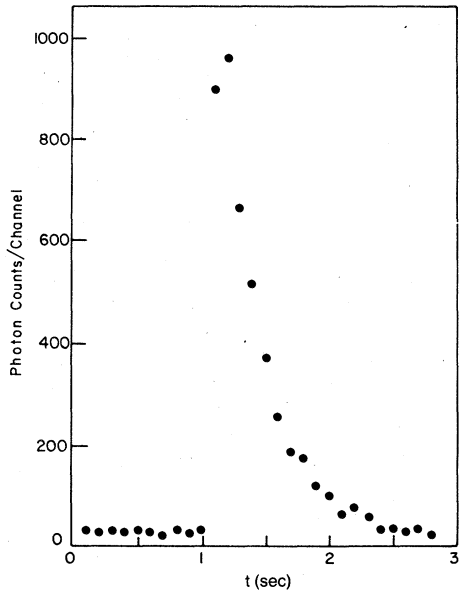


FIG. 2. Spontaneous $M1$ and laser-induced intercombination $E1$ decay signals from stored $Li^+$ ions. The small count rate between 0 and 1 sec is the spontaneous $M1$ emission; the laser beam is switched into the trap at $t=1$ sec and the resulting burst of 202-Å $E1$ photons is a measure of the number of metastable ions present.

scribed in this section.

To determine the time dependence of the metastable state, one can either observe the decay process (spontaneously emitted photons) or observe the number of undecayed metastable ions. Nonradiative quenching of the metastable state, discussed below, forced us to choose the latter method. The $Li^+$ energy levels relevant to this work are shown in Fig. 1. A cw dye laser at 5485 Å excites the $2\,^3S_1$-$2\,^3P_1$ transition. Relativistic effects, such as the spin-orbit interaction, mix $2\,^3P_1$ with $n\,^1P_1$ states[10] and result in a branching ratio of $\simeq 1:1200$ for an intercombination $2\,^3P_1$-$1\,^1S_0$ decay (202 Å) versus decay back to $2\,^3S_1$. With typical laser power ~50 mW, the entire metastable population is depleted in a time $\tau_1 \simeq 0.3$ sec, much less than the total metastable lifetime (determined primarily by nonradiative quenching) $\tau_m \simeq 5$ sec at an operating pressure of $10^{-9}$ torr. Thus each metastable ion is forced to emit a detectable 202-Å photon in a time period $\tau_l$, and since $\tau_l \ll \tau_m$, the number of photons counted is proportional to the number of metastables existing at the time when the laser is turned on. By varying the delay between creation and detection, the metastable time dependence is measured. Since the spontaneous emission count rate is roughly the same as the detector dark rate (~10 counts per minute), the ability to compress all photon counts into the short time period $\tau_l$ considerably enhances the signal-to-noise over the alternative method of measuring the time dependence by observing spontaneous decay. A typical set of data is shown in Fig. 2, where the photon counts are collected in 0.1-sec-wide bins. In this case spontaneous photons are counted for 1.0 sec, the laser beam is turned on at $t=1.0$ sec, and laser-induced depletion is then observed. The first channel after the laser comes on is artificially low owing to the time required ($\simeq$20% of a channel) to open the mechanical shutter which passes the laser beam.

By using this laser depletion technique, we established that the metastable population decays exponentially. A typical decay, using 1-sec-wide bins, is shown in Fig. 3, where the signal was followed for more than three lifetimes. The decay time also agrees well with decay times determined, under similar conditions, from spontaneous emission, though the poor signal-to-noise of the spontaneous-decay signal requires substantially longer collection periods to achieve comparable precision. From a comparison of metastable-ion decay curves collected both ways and measurement of the decay of the total stored charge, two important facts emerged. First, the metastable lifetime $\tau_m$ was much less than the ion storage lifetime. At a residual pressure $\simeq 1\times 10^{-9}$ torr, $\tau_m \simeq 5$ sec whereas the ion storage lifetime was typically 20 sec. Second, the integrated number of spontaneous counts was smaller, by roughly a factor of 10, than the integrated number of laser-induced counts. This is far too much to explain merely through storage losses and differences in

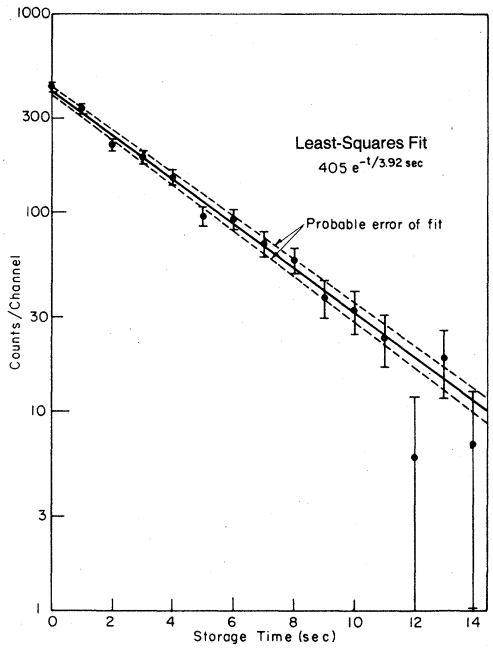


FIG. 3. Decay of integrated laser-induced $E1$ emission versus the time at which the laser beam is switched into the trap volume.

detection efficiencies. The most reasonable explanation for these observations is nonradiative quenching of the metastable ions by collisions with background gas molecules. This could cause most metastable ions to be lost without emitting a photon, so the integrated spontaneous count rate would be substantially less than if spontaneous emission were the only loss process.

Further information concerning the apparent quenching was obtained by measuring the number of ions stored with and without the laser on. With the laser on continuously, metastable ions are forced into the ground state very shortly after creation, and all ground-state ions exhibit the same storage loss rate. Without the laser, however, the faster loss rate of metastable ions could conceivably be to a neutral state, via charge capture, which would be lost from the trap. In that case, comparison at time $t=\tau_m$ of the number of stored ions with and without the laser would show a difference. The metastable fraction is estimated, based on counting rates and detector efficiencies, to be $\simeq 10\%$. No difference in the ion number was found, to an accuracy of 1%. This is consistent with a quenching process of the form

$$Li^+(2\,^3S_1)+X \rightarrow Li^+(1\,^1S_0)+X', \qquad (1)$$

where $X'$ is related to $X$ through a process such as Penning ionization, dissociation, or near-resonant charge capture to an autoionizing $Li(1s2snp)$ state[11]

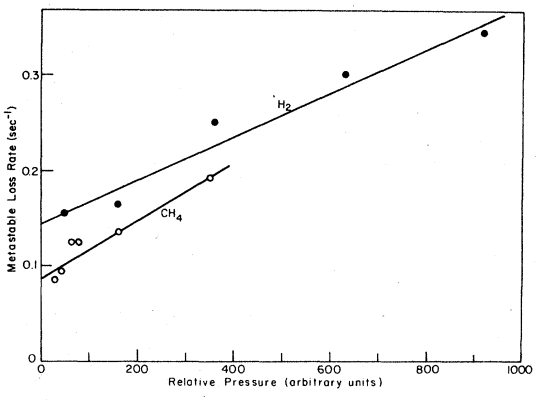


FIG. 4. Total loss rate of $2\,^3S_1$ $Li^+$ ions vs pressure of $CH_4$ and $H_2$ in the trap chamber. The pressure scale is uncalibrated; 100 pressure units is about $1\times10^{-9}$ Torr. The zero-pressure intercepts differ because the base pressure in the vacuum chamber was not the same when the two sets of data were collected.

which decays to $Li^+(1\,^1S_0)+e^-$ in $\leq 1$ $\mu$sec (before the neutral can escape from the trap).

Additional tests to verify that the metastable loss was due to collisional quenching were made by varying the background-gas composition and density. A residual-gas analyzer showed the principle components of the background gas to be $H_2$, $CH_4$, $H_2O$, CO, and $CO_2$. The metastable loss rate $\tau_m^{-1}$ as a function of relative pressure was measured for all of these except $H_2O$. Results for $H_2$ and $CH_4$ are shown in Fig. 4: CO and $CO_2$ behaved similarly. It was also observed that the ion storage time was independent of $H_2$ and $CH_4$ pressure over the range covered, and changed less rapidly than the metastable lifetime as the CO and $CO_2$ pressures were varied. This indicated the existence of a mechanism causing the preferential loss of metastable ions. The collisional-quenching cross sections were not determined since the residual-gas analyzer was not absolutely calibrated, but comparison with ion-guage readings and typical ionization efficiencies allowed an estimate of $\approx 10^{-14}$ cm$^2$ for the cross sections. These are not unreasonable for the processes mentioned above.

Summarizing these observations: (i) The metastable loss rate was exponential and faster than the ion loss rate from the trap; (ii) most of the metastable loss was not by the emission of a photon; (iii) most, probably all, of the metastable loss was to the ionic ground state; and (iv) the metastable loss rate was a sensitive function of the residual-gas pressure and composition. We concluded that the metastable time dependence could be explained by a combination of storage losses, spontaneous decay, and nonradiative quenching collisions.

To determine the rate of radiative decay only, the following scheme was used. One notes that, at any instant of time, the rate $dS/dt$ at which photons are emitted is related to the number $N$ of metastables by

$$\frac{dS(t)}{dt}=\frac{N(t)}{\tau_r}, \tag{2}$$

independent of any nonradiative losses which may also be occuring. A simultaneous measurement of $dS/dt$ and $N$ would allow the radiative lifetime $\tau_r$ to be determined. This is essentially the method used by Woodworth and Moos[6] in He. While a simultaneous and instantaneous measurement is not experimentally feasible, a sufficiently good approximation can be made. Consider the case where, following ion creation, a total $S_1$ of spontaneous $M1$ photons are counted for a time $T_1$, after which the laser is turned on and a total of $S_2$ spontaneous plus laser-induced photons are counted in a time interval $T_2$ during which all the metastables are depleted. Then for $T_1$ sufficiently small, and assuming no difference in detector efficiencies for the two photon wavelengths, one has simply

$$\tau_r=(S_2/S_1)T_1. \tag{3}$$

A more realistic expression is obtained from a detailed consideration of the several competing loss processes. Let the various loss rates be $\gamma_r=\tau_r^{-1}$ = the radiative decay rate, $\gamma_q=\tau_q^{-1}$ = the nonradiative loss rate, and $\gamma_l=\tau_l^{-1}$ = the laser depletion loss rate. While the laser is off, the total metastable decay rate $\gamma_m$ is given by

$$\gamma_m=\gamma_r+\gamma_q, \tag{4}$$

while with the laser on, the total depletion rate $\gamma_d$ is

$$\gamma_d=\gamma_r+\gamma_q+\gamma_l. \tag{5}$$

A measurement of the $2\,^3S_1$ population time dependence, such as shown in Fig. 3, gives $\gamma_m$. A least-squares analysis of the depletion itself, as in Fig. 2, gives $\gamma_d=\tau_d^{-1}$. One can write the rate equations for counting photons during time periods $T_1$ (laser off) and $T_2$ (laser on), respectively, as

$$\frac{dS_1}{dt}=\epsilon_{210}\gamma_r N_0 e^{-\gamma_m t}, \tag{6}$$

$$\frac{dS_2}{dt}=(\epsilon_{210}\gamma_r+\epsilon_{202}\gamma_l)N_0 e^{-\gamma_m T_1}e^{-\gamma_d t'}, \tag{7}$$

where $\epsilon_{210}$ and $\epsilon_{202}$ are the efficiencies for counting the 210-Å spontaneous photons and the 202-Å laser-induced photons, $N_0$ is the initial number of metastable ions, and $t'=t-T_1$. During $T_2$ we have included both spontaneous and laser-induced decay. These equations are easily integrated to give $S_1$ and $S_2$, the number of photons counted in $T_1$ and $T_2$. Eliminating $N_0$ and solving for the radiative lifetime yields

$$\tau_r=\frac{\epsilon_{210}}{\epsilon_{202}}\frac{\tau_m^2}{(\tau_m-\tau_d)}\left((e^{\gamma_m T_1}-1)\frac{S_2'}{S_1}-\frac{\tau_d}{\tau_m}\right), \tag{8}$$

where

$$S_2'=S_2/(1-e^{-\gamma_d T_2}) \tag{9}$$

is the number of photons which would be counted if $T_2\to\infty$. A small correction ($\leq 1\%$) is made to $S_2'$ to account for the finite time ($\approx$20 msec) at the beginning of $T_2$ needed for the mechanical laser beam shutter to open.

Equation (8) for the radiative lifetime of the $2\,^3S_1$ state depends only on measurable quantities and explicitly takes account of the nonradiative loss of the metastable ions. Section III describes the experimental details of measuring the needed quantities.

## III. EXPERIMENTAL METHOD

A basic requirement of this work is the ability to confine ions for many seconds in a volume from which decay photons may be collected, and which is accessible to the laser beam. This is accomplished with an rf-quadrupole ion trap,[12,13] consisting of two endcap electrodes and a ring electrode which are hyperboloids of revolution. A potential

$$U=U_0-V_0\cos\Omega t \tag{10}$$

is applied to the ring electrode. The equations of motion in the axial and radial directions are then Mathieu equations, and for a given ion charge-to-mass ratio, the motion is bounded for appropriate choices of $U_0$, $V_0$, and $\Omega$. The ion motion (time averaged over a few rf periods) can be described by an effective harmonic potential

$$\phi_{\text{eff}}=(r^2/r_0^2)D_r+(z^2/z_0^2)D_z, \tag{11}$$

where $r_0$ and $z_0$ are the inside radius of the ring electrode and half the spacing of the cap electrodes, respectively. $D_r$ and $D_z$ are the potential-well depths. In most cases, the trap was operated with a spherical potential well: $D_r=D_z=D$.

A block diagram of the experiment is shown in Fig. 5. The $Li^+$ ions are created by electron impact on a lithium atomic beam which passes through the center of the trap. Passage of the beam is controlled by a solenoid-actuated beam flag. A $\frac{1}{4}$-in.-diam dispenser cathode mounted axially 2–3 mm behind a wire grid in the surface of the lower endcap provides an electron-beam current of about 30 $\mu$A. A 1-sec-long filling per-

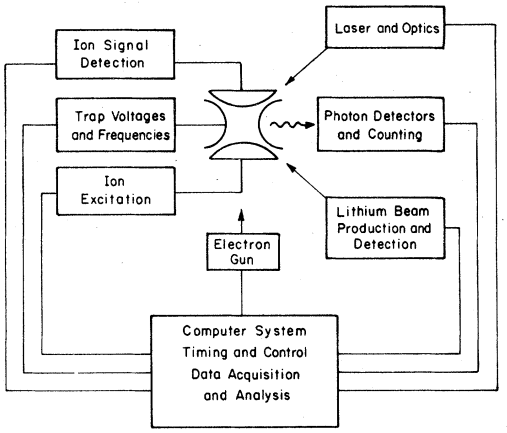


FIG. 5. Block diagram of the experiment.

iod produces a maximum ion number of $\approx 2\times 10^5$. A residual-gas pressure $\approx 1\times 10^{-9}$ torr allows the ions to be stored with a mean lifetime of $\approx$20 sec and a nonradiative collisional-quenching time for the metastables $\tau_m \approx 5$ sec.

The trap itself has dimensions $r_0 = z_0 = 3.0$ cm. The endcap electrodes are accurately machined oxygen-free high-conductivity (OFHC) copper, while the ring electrode is a copper wire mesh, formed on a template, which allows good optical access to the trap interior. The rf voltage is at frequency $\Omega = 2\pi \times 1.0$ MHz and amplitude $V_0 = 250$–400 V. A dc bias $U_0 = 0$–30 V is used to produce spherical potential wells in the range $8 \leq D \leq 18$ V.

A sideband excitation-resonant detection method is used to monitor the number of stored ions.[12] The ion axial motion in the potential well $\phi_{\text{eff}}$ is harmonic at frequency $\omega_z$; superimposed upon this is a small-amplitude micromotion at the rf drive radio frequency $\Omega \gg \omega_z$. A spectral decomposition of the total motion thus contains frequencies $\Omega \pm \omega_z$ as well as $\omega_z$. Excitation at the sideband frequency $\Omega + \omega_z$ causes the entire ion cloud to oscillate coherently at frequency $\omega_z$. In practice, the excitation frequency is fixed at $\Omega + \omega$ and a dc ramp voltage applied to the ring electrode sweeps the ion frequency $\omega_z$ through resonance with $\omega = 2\pi \times 100$ kHz. A tuned amplifier detects the ion cloud oscillation at $\omega$ and produces an output signal proportional to the number of ions. The signal height is automatically recorded by a peak detector circuit, digitized, and stored in the computer.

A study of the ion distribution was useful for understanding the details of the ion-cloud–laser-beam interaction. This was done by measuring the $2\,^3P_1$-$1\,^1S_0$ intercombination signal as a function of the laser beam position as it was rapidly scanned across the ion cloud.[14] The results of these measurements showed that the metastable ions in spherical wells $8 \leq D \leq 18$ eV have a Gaussian density distribution

$$n = n_0 e^{-(r/\delta)^2},$$

with $\delta \approx 0.6$ cm. This is consistent with a Maxwellian distribution of ion energies with a temperature of $\approx$5000 K.

The laser is a cw dye laser using rhodamine-110 dye; when tuned with a three-element birefringent filter alone, the laser has a linewidth $\delta\lambda \approx 0.2$ Å. Installation of a 200-GHz free-spectral-range etalon in the laser cavity reduces the linewidth to $\approx$0.02 Å, allows fine tuning, and greatly improves the wavelength stability. Output power under these conditions is typically 50–100 mW. The wavelength is monitored by scanning a portion of the beam across an external etalon and displaying the transmitted intensity, detected by a photodiode, on an oscilloscope. Stability during a 1-h data-collecting period was generally better than $\pm$0.01 Å; variations of this size do not affect the measurement of $\tau_r$. The laser beam is directed perpendicular to the $z$ axis in the trap midplane. Before entering the vacuum chamber, the linearly polarized laser beam passes through a polarization rotator which establishes the desired polarization orientation with respect to the trap $z$ axis. An optional telescope can expand the beam from its normal diameter of $\approx$1 mm up to $\approx$4 cm.

Xuv photons are detected by two EMI venetian-blind electron multipliers located 180° apart in the trap horizontal midplane. Grazing-incidence light pipes, coated with 200-Å-thick platinum, are located in front of the detectors and improve the photon collection by an estimated factor of $\approx$7.5. An 800-Å-thick, 1-in.-diam aluminum-foil filter is also located directly in front of the first dynode of each multiplier to prevent escaping ions or metastable neutrals from being counted. Transmission[15] of the foils is $\approx$65% for photons of wavelength 200 Å. The detector output pulses are amplified, passed through a discriminator, and accumulated by the computer. Adjustment for optimal signal-to-noise leaves a residual dark rate from the two detectors combined of $\approx$10 counts/min.

An important parameter of the detectors is the relative efficiency factor $\epsilon_{202}/\epsilon_{210}$. This was measured by comparing our detectors, with aluminum foils in place, to an absolutely calibrated channeltron electron multiplier.[16] A Ne discharge source and a 2.47-m vuv grazing-incidence monochromator provided nine peaks in the wavelength range 196–228 Å, which were used for the calibration. While the absolute efficiency of the channeltron has a 13% uncertainty, the relative efficiency at

two wavelengths in this range, the only factor needed in this work, was conservatively estimated to have a 4% uncertainty. Combined with a 3% measurement error and a 3% error from a least-squares analysis, the total error in our determination of $\epsilon_{202}/\epsilon_{210}$ is estimated to be 6%. (Both detectors were calibrated separately and produced the same result.) The value obtained was $\epsilon_{202}/\epsilon_{210} = 0.87 \pm 0.05$, where the error is one standard deviation.

The control and data collecting for the entire experiment was performed by a PDP-11 computer. For the purpose of storing data, the computer functions essentially as a multichannel analyzer. The timebase used during data collection was a 60-Hz line clock. Additionally, the computer monitors whether the laser is tuned to the center of the $2\,^3S_1$-$2\,^3P_1$ resonance; any decrease in the integrated laser-induced photon counts, normalized to the number of ions, is noted on the teletype and allows fine tuning of the laser wavelength. Either upon operator command or when a preset number of cycles is completed, the computer prints the data and branches to an analysis program.

According to Eq. (8), the quantities needed to determine $\tau_r$ are $S_1$, $S_2$, $\tau_d$, and $\tau_m$. These are found in a three-stage process. First, $\tau_m$ is measured using the laser depletion technique, as shown in Fig. 3, with several different delays between the trap filling and the laser beam shutter opening. A least-squares fit of an exponential decay to these data yields $\tau_m$ and $\sigma(\tau_m)$, its standard deviation. Second, data are collected in the manner shown in Fig. 2 in order to determine $S_1$ from the spontaneous counts and $S_2$ and $\tau_d$ from the laser-induced counts. A study of the signal-to-noise obtained in a given time period indicated that optimally $T_1 \approx \frac{1}{2}\tau_m$ and that $T_2$ should be several times $\tau_d$ in order to have the laser depletion proceed to completion. Most data were taken with $T_1 = 2.0$ sec and $T_2 \approx 5\tau_d \approx 2$ sec. The data-analysis program returns $\tau_d$ and $\sigma(\tau_d)$ from a least-squares analysis as well as $S_1$ and $S_2$, defined in Eq. (9). Third, $\tau_m$ is remeasured as in the first step and the two values are averaged to obtain a best estimate for its value during the measurement of $S_1$, $S_2$, and $\tau_d$. Finally, $\tau = (\epsilon_{202}/\epsilon_{210})\,\tau_r$ is computed using Eq. (8). The values of $\sigma(\tau_m)$ and $\sigma(\tau_d)$, returned from the least-squares programs, along with the statistical uncertainties for $S_1$ and $S_2$, are used to calculate the standard deviation $\sigma(\tau)$ of $\tau$. The entire process typically takes about an hour to achieve a 10% measurement.

## IV. RESULTS

Data were collected separately for the isotopes $^6Li^+$ and $^7Li^+$. The sample of $^7Li$ was >99.9% $^7Li$, but the $^6Li$ was in fact 95.6% $^6Li$ and 4.4% $^7Li$. Thus when studying $^6Li^+$, the small number of $^7Li^+$ ions contribute to the spontaneous photons but not to the laser-induced photons, since the $2\,^3S_1$-$2\,^3P_1$ transition in $^7Li^+$ is isotopically shifted away from the $^6Li^+$ transition to which the laser was tuned. This requires a correction:

$$\tau(^6Li^+ \text{ corrected}) = 1.046 \times \tau(^6Li^+ \text{ uncorrected}).$$

The weighted averages, isotopically corrected, of 26 runs for $^6Li^+$ and 33 runs for $^7Li^+$, without the detector efficiency factor, are

$$\tau(^6Li^+) = 49.9 \pm 1.0 \text{ sec}, \quad \tau(^7Li^+) = 52.0 \pm 0.9 \text{ sec}. \tag{12}$$

The errors quoted here are $1\sigma$ errors of the mean, representing only the statistical error involved in determining $\tau_r$. Possible systematic errors are discussed below. The spread of the measurements is indicated by the standard deviations of the distributions of data:

$$\sigma(^6Li^+) = 4.2 \text{ sec and } \sigma(^7Li^+) = 5.1 \text{ sec}.$$

One potential source of systematic error arose from the background subtraction method. The measurements of $S_2$, $\tau_d$, and $\tau_m$ are not particularly sensitive to the background subtraction since the laser-induced count rate was considerably higher than the background. The spontaneous photon rate, on the other hand, was roughly the same as the background rate, so errors in the background subtraction procedure could seriously affect $S_1$. Two methods were studied. In the first, a background cycle identical to each data cycle was taken except that the ion-trap dc potential was switched very negative during the fill period in order not to store $Li^+$ ions. The second method differed in that $Li^+$ ions were excluded simply by not opening the lithium beam flag during the fill period; the dc trap voltage was held constant. An analysis of data collected by these two methods indicated a possible variation of ≈2% in the final value for $\tau_r$. The second method was judged preferable, both because it stores any background gas ions, which are usually stored during the data cycle, and because the first method causes slightly different electron trajectories during the fill period that might alter any charging of detector surfaces. All data used in the weighted averages utilized the second method, and a possible systematic error of 2% is assigned.

A general search for systematic errors covered numerous possibilities. The residual-gas composition and pressure were varied; this should not affect the result if the analysis leading up to Eq. (8) is correct. We admitted $H_2$, $CH_4$, $H_2O$, CO,

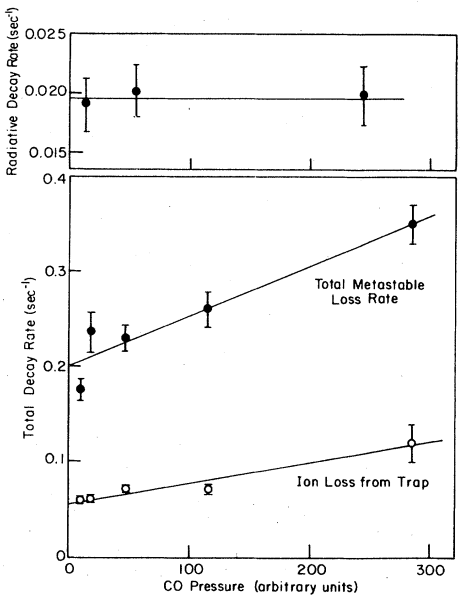


FIG. 6. Ion-storage loss rate, total metastable loss rate, and metastable radiative decay rate vs pressure of CO. 100 pressure units is about $1\times10^{-9}$ Torr.

and air through a leak valve and measured $\tau_r$ as the partial pressure of each was varied up to at least ten times its base value. No effect on $\tau_r$ was observed. The storage loss rate, the total metastable loss rate, and the radiative rate as a function of CO pressure are shown in Fig. 6. Data for the other gases were similar.

A possible source of excess counts which would not be compensated for during the background cycle is the presence of small holes in the aluminum-foil filters. This possibility was checked by looking for counts above the background long after the metastable population had been laser depleted but before many ground-state ions had been lost. The integrity of the foils remained good throughout the five-month period in which data were accumulated.

Since the ion trap is somewhat mass selective, the percentage of $^7Li^+$ ions stored during the $^6Li^+$ runs may not have been the same as its 4.4% composition in the bulk lithium. We observed an ion signal from the $^7Li^+$, using the electronic detection discussed in Sec. III, but it was too noisy to compare quantitatively with the $^6Li^+$ signal. We estimate the error in $\tau_r(^6Li^+)$ from this source to be $\leq 2\%$. A possible error in $\tau_r(^7Li^+)$ only occurs due to the fact that we took most of the $^7Li^+$ data without using the internal etalon in the laser. This was because the larger hyperfine structure in $^7Li^+$ made it difficult to keep $\tau_l < 1$ sec with the narrow laser linewidth. The larger linewidth achieved by using only the birefringent filter in the laser alleviated this problem but could lead to an error $\leq 2\%$ in $\tau_r(^7Li^+)$ because of slight wavelength drifts during the data collection. Another possible error related to the laser is the effect of the beam size. Since the spontaneous photons originate from the entire ion cloud but laser-induced photons come only from the region of the laser beam, a difference in the geometrical collection efficiencies could occur. By expanding the laser beam with a telescope, we have put 3% limits on any error arising from this source.

A more serious systematic problem concerns the trap well depth and the electron energy. It was initially observed that well depths $D = 18$ eV with electron energies $E_{elec} < 300$ V generally resulted in smaller values for $\tau_r$ than did either well depths $D = 8$ eV or $E_{elec} > 300$ V with $D = 18$ eV. Furthermore, there was little, if any, dependence on $E_{elec}$ for $E_{elec} > 300$ V. We concluded that the stronger rf fields at $D = 18$ eV were seriously perturbing the trajectories of lower-energy electrons, causing trap surfaces and the detectors to charge up slightly during the fill period, and leading to systematic errors. With either smaller rf fields or larger electron energies, the electron trajectories are more nearly straight lines through the trap center, and this problem diminishes. All data included in the final results used $E_{elec} > 300$ V (usually 450 V); the error from this source is judged to be less than 5%.

A final point to consider is the effect of optical pumping of the $2\,^3S_1$ ions. The principal concern is that an alignment of the $2\,^3S_1$ state would result in anisotropic photon emission and cause a systematic error in $S_2$. The major parameters affecting optical pumping are the magnetic field and the angle of laser polarization with respect to the field. As is well known,[17] the induced dipole created by the laser's electric field is destroyed by a uniform magnetic field when the precession frequency of the dipole exceeds the radiative decay rate (magnetic depolarization). The pertinent condition for magnetic depolarization is

$$\alpha = \mu_B B/h\gamma \gg 1, \tag{13}$$

where $B$ is the field strength, $\gamma$ is the radiative decay rate, and $\mu_B$ is the magnetic moment of the excited state. Our experiment uses an axial magnetic field $\approx 50$ G to help focus the electron beam. For the case of $2\,^3P_1$ in $Li^+$ this gives $\alpha \approx 20$, so magnetic depolarization should be complete. One can further show that, for the case of complete magnetic depolarization, a laser beam polarization at an angle $\theta = \cos^{-1}(1/\sqrt{3}) \approx 54°$ with respect to the magnetic field will produce a uniform distribution of substate population.[17] We have substantiated this by detailed optical-pumping calcu-

TABLE I. Summary of measurements and error analysis. Raw data average times calibration factor (times isotope factor for $^6Li^+$).

$^6Li^+$: $\tau_r = 57.4$ sec.
$^7Li^+$: $\tau_r = 59.8$ sec.
Average: $\tau_r = 58.6$ sec.

| Error source | Fractional contribution |
|---|---|
| Detector calibration | 6% |
| Well depth, electron energy | 5% |
| Background subtraction | 2% |
| Incomplete magnetic depolarization | 2% |
| Laser beam polarization angle | 2% |
| Laser beam size | 3% |
| $^6Li^+$: isotope correction<br>$^7Li^+$: laser wavelength drift | 2% |
| Maximum systematic error | 22% |
| Statistical error | 2% |
| 95%-confidence error estimate: | 22% |
| Result: $\tau_r = 58.6 \pm 12.9$ sec. | |

lations as a function of laser wavelength and polarization. Our calculations are in good agreement with observation. A report of these fluorescence studies will be published separately.

By maintaining $B \geq 50$ G and $\theta = 54°$ during the collection of all data used for determining $\tau_r$, an isotropic distribution of photons was assured. We have assigned systematic errors of 2% to possibly incomplete magnetic depolarization and 2% to a possible error of a few degrees in $\theta$. Since electron impact excitation could produce some alignment of the initial population of $2\,^3S_1$ ions, leading to an anisotropic $M1$ decay pattern, some data were taken after an initial brief laser pumping period was used to establish a uniform population of the $2\,^3S_1$ substates. No significant differences were noted between values of $\tau_r$ obtained with and without this initial laser pumping.

The results of our data averaging and error analysis are shown in Table I. An average of the $^6Li^+$ and $^7Li^+$ data yields a value of 58.6 sec for the radiative lifetime. The assignment of an appropriate error to this result was done as follows. The errors shown in Table I are, with the exception of the 2% statistical, error, estimates of unresolved systematic errors. Their effect on the result is always the same, but we cannot correct for them since we do not know the correct sign for each. Our approach is to consider the worst case; i.e., where all systematic errors affect $\tau_r$ in the same way. Thus we add these error estimates and regard the result as a 95%-confidence-level

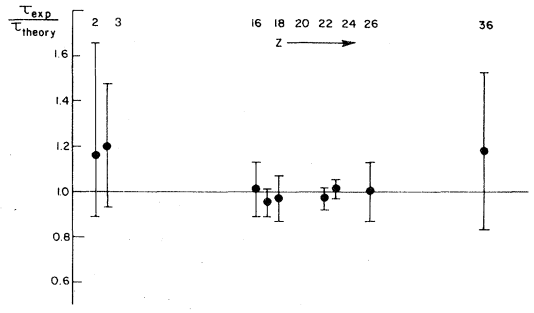


FIG. 7. Ratio of experimental to theoretical radiative lifetime values for the $2\,^3S_1$ state vs $Z$. Theoretical values used are from Refs. 4 and 5. The experimental value at $Z = 2$ is from Ref. 6 and those used at $Z = 16$ and higher are summarized in Ref. 7. This work provides the value at $Z = 3$.

estimate of the magnitude of unresolved systematic effects. We combine this systematic error in an rms fashion with the statistical error to achieve our final error estimate. The 12.9-sec error deduced in this manner does not differ significantly from a $2\sigma$ error of 11.7 sec found by rms combination of all the error estimates and the statistical error. The final result is then

$$\tau_r = 58.6 \pm 12.9 \text{ sec.}$$

## V. DISCUSSION

Figure 7 shows a comparison of measured and theoretical values of $\tau_r$ for $Z$ ranging from 2 to 36. All of the error bars in this figure represent 95%-confidence levels in the experimental values. Considering that the lifetimes measured have spanned nearly 14 orders of magnitude, the general agreement of theory and experiment is impressive. Still, it is somewhat disturbing that both $Z = 2$ (He) and $Z = 3$ ($Li^+$) require $2\sigma$ error bars to reach agreement, and both experimental lifetimes are longer than theory predicts. Since the theoretical radiative decay rate scales as $Z^{10}$, any other process scaling with a lower power of $Z$ could be a contributing factor at low $Z$, while not observed in the higher-$Z$ beam-foil experiments. No theoretical hypothesis has been advanced, though, for any mechanism which would inhibit the decay. Obvious competing processes, such as hyperfine induced decays, could only shorten the lifetime, and they are easily estimated to be several orders of magnitude too small to be of importance. Further work, both experimental and theoretical, would not be without merit as long as the puzzle remains of nonexponential behavior at high $Z$ and possibly longer-than-theoretical lifetimes at low $Z$.

ACKNOWLEDGMENTS

We wish to express our gratitude to Drs. F. Paresce and S. Bowyer of the University of California Space Sciences Laboratory for the use of their xuv calibration facility. This work was supported by the Chemical Sciences Division Office of Basic Energy Sciences, U. S. DOE, under Contract No. W-7405-Eng-48.

---

*Present address: Center for Astrophysics, 60 Garden St., Cambridge Mass. 02138.

[1]A. H. Gabriel and C. Jordan, Nature (London) 221, 947 (1969).
[2]G. Breit and E. Teller, Astrophys. J. 91, 215 (1940).
[3]H. R. Griem, Astrophys. J. 156, L103 (1969).
[4]G. W. F. Drake, Phys. Rev. A 3, 908 (1971).
[5]W. R. Johnson and C. Lin, Phys. Rev. A 9, 1486 (1974).
[6]J. R. Woodworth and H. W. Moos, Phys. Rev. A 12, 2455 (1975).
[7]The theory and measurements are summarized by R. Marrus and P. J. Mohr in *Advances in Atomic and Molecular Physics, Volume 14*, edited by D. R. Bates and B. Bederson (Academic, New York, 1978).
[8]D. L. Lin and L. Armstrong, Jr., Phys. Rev. A 16, 791 (1977).
[9]F. F. Freemen, A. H. Gabriel, B. B. Jones, and C. Jordan, Philos. Trans. R. Soc. London A 270, 127 (1971).
[10]G. W. F. Drake and A. Dalgarno, Astrophys. J. 157, 459 (1969).
[11]P. Hvelplund, J. Phys. B 9, 1555 (1976).
[12]H. G. Dehmelt, Adv. At. Mol. Phys. 3, 53 (1967); 5, 109 (1969).
[13]R. D. Knight, Ph.D. thesis, University of California, Berkeley, 1979 (Lawrence Berkeley Laboratory Report No. LBL-9082) (unpublished).
[14]R. D. Knight and M. H. Prior, J. Appl. Phys. 50, 3044 (1979).
[15]W. R. Hunter, D. W. Angel, and R. Tousey, Appl. Opt. 4, 891 (1965).
[16]J. E. Mack, F. Paresce, and S. Bowyer, Appl. Opt. 15, 861 (1976).
[17]A. Mitchell and M. Zemansky, *Resonance Fluorescence and Excited Atoms* (Cambridge University, London, 1934).